Electronic Spin Transition in Nanosize Stoichiometric Lithium Cobalt Oxide

Danna Qian,[†] Yoyo Hinuma,[†,‡] Hailong Chen,[§] Lin-Shu Du,[∥] Kyler J. Carroll,[†] Gerbrand Ceder,[§] Clare P. Grey,[∥,⊥] and Ying S. Meng*,[†]

[†]Department of NanoEngineering, University of California San Diego, La Jolla, California 92109, United States

[‡]Department of Materials Science and Engineering, Kyoto University, Kyoto, Kyoto, 606-8501, Japan

[§]Department of Materials Science and Engineering, Massachusetts Institute of Technology, Cambridge, Massachusetts 02142, United States

[∥]Department of Chemistry, University of New York at Stony Brook, Stony Brook, New York 11794, United States

[⊥]Department of Chemistry, Cambridge University, CB2 1EW, U.K.

ⓈSupporting Information

ABSTRACT: A change in the electronic spin state of the surfaces relevant to Li (de)intercalation of nanosized stoichiometric lithium cobalt oxide $LiCo(III)O_2$ from low-spin to intermediate and high spin is observed for the first time. These surfaces are the ones that are relevant for Li (de)-intercalation. From density functional theory calculations with a Hubbard U correction, the surface energies of the layered lithium cobalt oxide can be significantly lowered as a consequence of the spin change. The crystal field splitting of Co d orbitals is modified at the surface due to missing Co—O bonds. The electronic spin transition also has a significant impact on Co(III)−Co(IV) redox potential, as revealed by the change in the lithium (de)intercalation voltage profile in a lithium half cell.

Lithium cobalt oxide ($LiCoO_2$) is a compound of great importance, as it has been the most widely used positive electrode material for lithium ion batteries for nearly two decades. $LiCoO_2$ adopts the α-$NaFeO_2$-type crystal structure with rhombohedral symmetry (space group $R\bar{3}m$) and Li^+ and Co^{3+} ions sitting in octahedral sites formed by alternating layers of oxygen. Because of such an ordered layered structure, Li^+ can be reversibly deintercalated and reintercalated from $LiCoO_2$ to $Li_{0.5}CoO_2$ with a high electrochemical potential of up to 4.2 V (vs Li^+/Li). In recent years, it has been demonstrated that ultrafast charge/discharge rate capabilities can be achieved in this compound when nanoscale (<50 nm) particles with a morphology optimal for Li intercalation are prepared and tested.[1,2] Okubo et al.[1,3] observed several interesting phenomena associated with their nanosized $LiCoO_2$: First, lattice parameter expansion is observed in particles less than 20 nm in size; second, the magnetic susceptibility increases dramatically when compared with that of bulk-$LiCoO_2$. The authors hypothesized that these phenomena are mainly due to the presence of Co^{2+} on the surface of their nano-sized particles, Co^{2+} being present in the form of $Li_{1+x}Co^{2+}_x$-$Co^{3+}_{1-x}O_2$, as a consequence of their hydrothermal synthetic process. However, the interpretation of the magnetic data is ambiguous since no direct evidence for the presence of Co^{2+} was obtained.[3] Moreover, Levasseur et al.[4] pointed out that, in bulk

lithium overstoichiometric ("Li excess") samples, the charge is compensated by oxygen vacancies. This leads to some cobalt ions being in a square based pyramidal site with an intermediate spin (IS) configuration. In this communication we show that, for stoichiometric nanosized $LiCoO_2$, the anomaly in magnetic susceptibility can similarly be explained by the presence of IS or HS Co^{3+}, a phenomenon which alters the lithium (de)intercalation voltage significantly.

The surface energies of $LiCoO_2$ were calculated from first principles with the Hubbard U correction on the generalized gradient approximation (GGA+U) to the density functional theory (DFT). The results are listed in Table 1, and the specific

Table 1

surface	coordination no. of oxygen	γ (mJ/m²) ref 5 with LS	γ (mJ/m²) this work with LS	γ (mJ/m²) this work spin trans.
{104}	5/6	1048	1118	312
{110}	4/6	2241	2227	1241

details of the models are presented in the Supporting Information, section S1. We find that the surface energies are minimized when the surface Co^{3+} ions are in either the intermediate (IS) or high spin (HS) state depending on the crystallographic orientation. This change in the electronic spin state on the surface can be rationalized by a change in the surface Co crystal field due to the missing Co—O bonds.

$LiCoO_2$ particles are typically dominated by the {001} surface; however this surface is not active for Li (de)intercalation. Therefore, we focus on studying the {104} and {110} surfaces, which are the two lowest energy nonpolar surfaces identified by previous work.[5] Figure 1a shows the {104} surface of $LiCoO_2$, which represents a major, low energy surface for $LiCoO_2$; this surface slices through the Co, O, and Li planes and is expected to be involved in the (de)intercalation process. This represents the {100} surface of the NaCl lattice from which the ordered rocksalt $LiCoO_2$ is derived. In the bulk, and on the {001} surface, octahedrally coordinated Co^{3+}
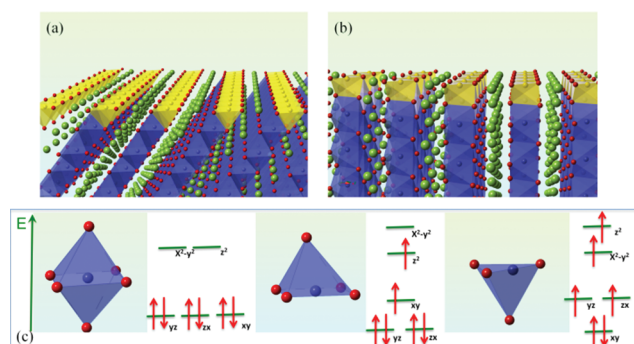
Figure 1. (a) {104} and (b) {110} surfaces of LiCoO$_2$. (c) Octahedrally, square pyramid and pseudotetrahedrally coordinated Co ions (red, oxygen; green, lithium; blue, Co).

ions are in the low spin (LS) state and do not have unpaired electrons. On the {104} surface, however, the Co^{3+} ions are coordinated by five oxygen ions, resulting in a square pyramidal configuration. The surface energy is then lowered significantly when going from the LS configuration (1118 mJ/m^2) to the IS (312 mJ/m^2). Figure 1b depicts the {110} surface of LiCoO$_2$. In this orientation, the Co^{3+} ions on the surface are coordinated by four oxygen ions with a pseudotetrahedral configuration. The surface energy is minimized from 2227 mJ/m^2 (LS) to 1241 mJ/m^2 (HS). The details of the crystal field splitting of 3d orbitals and the corresponding energy levels of bulk and surface cobalt ions are shown in Figure 1c. A square pyramidal crystal field breaks the degeneracy of both the t$_{2g}$ and e$_g$ orbitals observed for octahedral symmetry, since the missing O ion along the z-direction reduces the repulsion between 2p electrons and 3d electrons in orbitals pointing toward or closer to the z-axis. A pseudotetrahedral crystal field with two missing bonds in the xy plane leads to lower energies for the 3d$_{xy}$ and 3d$_{x^2-y^2}$ orbitals. A charge density plot, which represents the difference in up and down spins, of the {104} surface clearly shows the unpaired electrons as compared to the case of Co^{3+} (LS) in the bulk of LiCoO$_2$ (see Figure 2a and 2b).
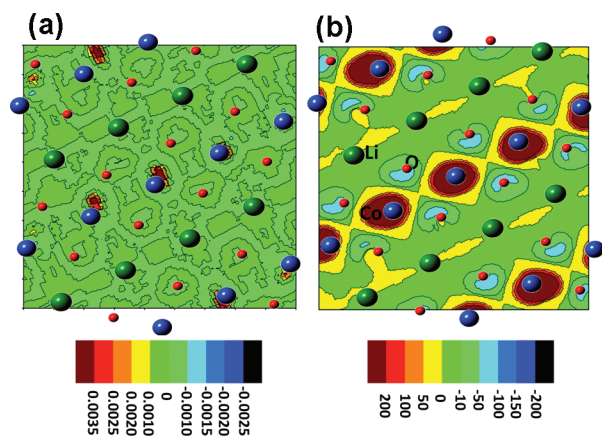
Figure 2. Spin density plot of the {104} plane of the bulk (a) and the surface (b). (Notice the scale differences in the spin density.)

The first principles calculations reveal that both the {104} and {110} surfaces with optimized Co coordination environments and electronic states expand normal to the surface, the displacement being on the order of 0.1−0.2 Å. It is important to point out that such changes in electronic spin states are also seen in first principles simulations of surfaces of CoO and Co$_2$O$_3$, as well as LiNiO$_2$.

To validate the hypothesis that the Co^{3+} on the surface is in an intermediate spin state by experimental spectroscopic techniques, stoichiometric LiCoO$_2$ samples with extremely small particle sizes (thus very large surface areas) provide the best opportunities. However, it is difficult to make stoichiometric nanoparticles of LiCoO$_2$ by conventional solid state or hydrothermal methods.[6] Okubo et al. reported samples with small particle sizes (8 to 32 nm), but the samples are most likely overstoichiometric, i.e., Li$_{1+x}$CoO$_2$.[1] By contrast, the molten salt method reported earlier[2] represents a much better approach to prepare stoichiometric LiCoO$_2$ nanoparticles. In this work, stoichiometric LiCoO$_2$ with very small particle sizes (10, 16, 20, 30, and 40 nm) were synthesized by using a modified molten salt method based on the previously reported method (see Supporting Information, section S2). We observed expansion of the lattice parameters from Rietveld analysis of the XRD results, similar to that observed by Okubo et al.,[1] along with magnetic susceptibility data that indicate the presence of unpaired electrons. X-ray diffraction (XRD) data indicate the formation of pure single-phase LiCoO$_2$ for the 20, 30, and 40 nm samples, with all the peaks corresponding to the layered α-NaFeO$_2$ structure (Figure 3a).
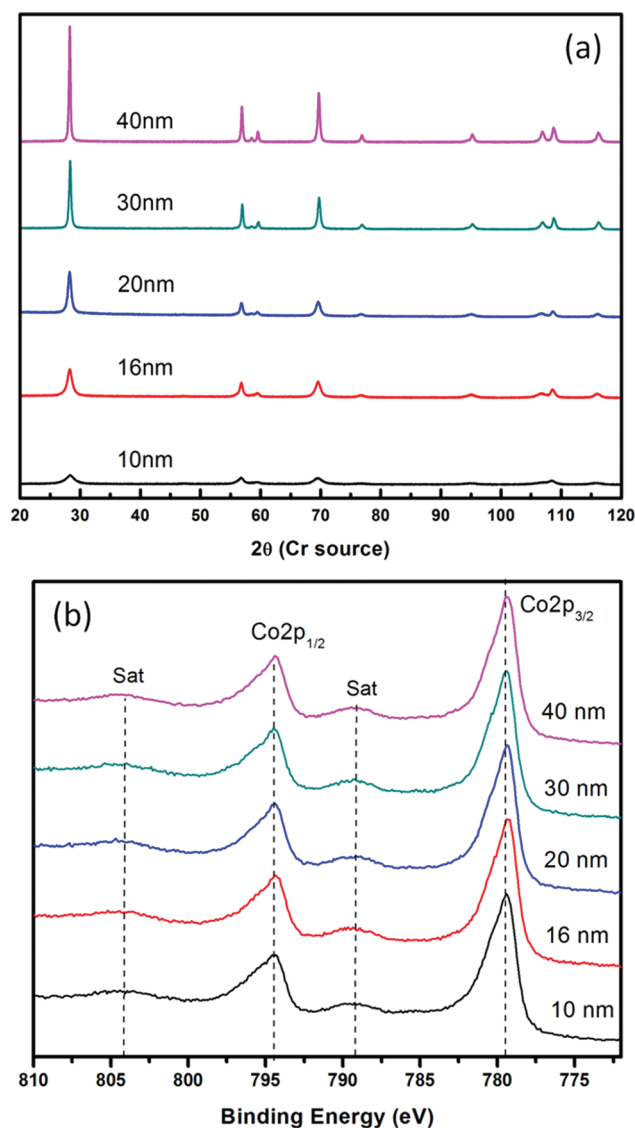

Figure 3. (a) XRD and (b) XPS spectra of nanosized stoichiometric LiCoO$_2$.

Lattice parameters are extracted and the c/a ratio is approximately 4.99, indicating a well-formed layered structure.[7] Detailed information regarding the lattice parameters is given in the Supporting Information, section S3. The reflections in the XRD pattern for the 10 nm particles are broad, and a quantitative refinement could not be achieved.

X-ray photoelectron spectroscopy (XPS) was carried out with a Thermo-Scientific K-Alpha spectrometer using a focused monochromatic Al Kα anode source (see Supporting Information, section S4). As shown in Figure 3b, all compounds show a Co $2p_{3/2}$ main peak at 779.5 eV with a satellite peak at 789.5 eV and a Co $2p_{1/2}$ main peak at 794.5 eV with a satellite peak at 804.5 eV. This observation confirms that the oxidation state is Co^{3+}. This is strong evidence that our nanosized $LiCoO_2$ samples are stoichiometric. Co^{2+} coordinated by oxygen is characterized by a strong broadening of the main line and a very intense satellite peak at 785.5 eV ($Co\ 2p_{3/2}$) and 802.5 eV ($Co\ 2p_{1/2}$),[6,8] which are both absent in the spectra.

^{7}Li magic-angle-spinning (MAS) NMR spectroscopy was performed at a magnetic field strength of 4.7 T with a spinning speed of 35 kHz to explore the Li nonstoichiometry in nanosized $LiCoO_2$. Figure 4a shows that the spectra of the
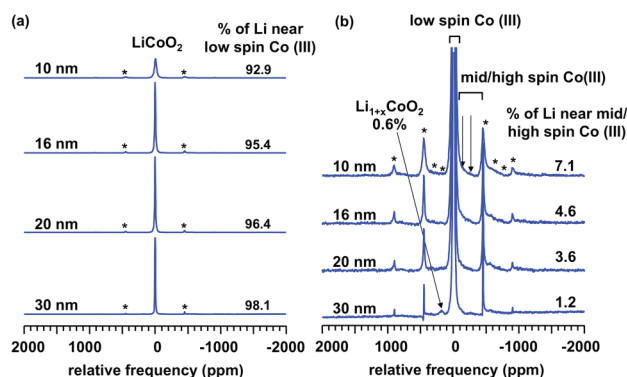

Figure 4. ^{7}Li MAS NMR spectra of $LiCoO_2$ with varying particle sizes. (a) Percentages of the Li near by low spin Co(III) in $LiCoO_2$ are listed in (a). Peak assignment and percentages of Li ions in environments nearby paramagnetic ions can be found in enlarged spectra. (b) Asterisks denote spinning sidebands.

10 to 30 nm particles are dominated by a single resonance at 0 ppm, as expected for a stoichiometric, diamagnetic $LiCoO_2$ sample.[4] The larger NMR line width observed for the 10 nm sample compared to the others may be due to the presence of a trace amount (<1%) of Co_3O_4 impurity, which results in faster transverse relaxation leading to a larger line width. A weak, hyperfine shifted resonance is observed at +185 ppm for the 30 nm sample. This shift, along with peaks at 3, −6, −16, and −40 ppm (not observed in our system here, presumably because they are too weak) were previously suggested to be associated with excess Li ions that replace Co^{3+} sites in the bulk, resulting in a defect structure discussed above, with two adjacent square-based pyramids containing two intermediate-spin Co^{3+} ions per oxygen vacancy.[4] Even in the 30 nm sample, the percentage of excess Li is only approximately 0.6%. Two new hyperfine-shifted resonances were observed at −115 and −260 ppm (Figure 4b), which are attributed to the presence of intermediate and/or high spin Co^{3+} (IS, HS). To the best of our knowledge, these shifts have not been reported in the literature. An analysis of the spin density on the {104} surface, as shown in Figure 2b, indicates that the Li$^+$ ions on this surface contain negative spin density and will thus give rise to a negative

shift. Integration of the spin density around the Li nucleus to 0.8 Å, using the approach developed by Carlier et al.,[9] confirms this observation and indicates that the Li nuclei in the subsequent {104} surface is negative, while the spin density of the Li in the layer below is smaller, but positive (and thus it may be difficult to resolve from the intense bulk $LiCoO_2$ resonance/and or be buried under the spinning sidebands). Further calculations will focus on the direct calculations of hyperfine shifts[10,11] on this and a wider range of surfaces. Importantly, quantitative fitting of the NMR spectra to extract the concentration of Li$^+$ ions nearby paramagnetic Co ions confirms that the percentage of paramagnetic ions increases with decreasing particle size (Supporting Information, section S5).

Magnetic measurements were performed, using a superconducting quantum interference device (SQUID), at a magnetic field of 1.0 T in the temperature range 5−300 K. The molar magnetic susceptibility of the various sized nano-$LiCoO_2$ particles are plotted as a function of temperature in Figure 5a. The magnetic susceptibility
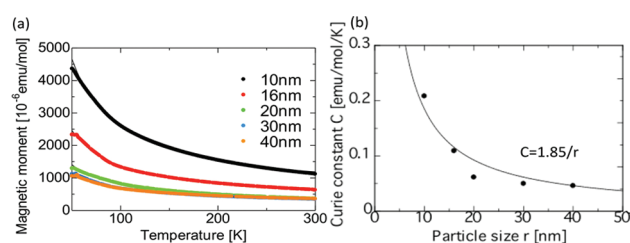
Figure 5. (a) Molar magnetic susceptibilities of particle size 10, 16, 20, 30, and 40 nm samples as a function of temperature. (b) The Curie constants of these samples determined from the $1/\chi$ vs T. (Both are measured with sample holder corrected.)

of bulk $LiCoO_2$ is low and practically temperature independent, which is attributed to a Van Vleck type of paramagnetism associated with diamagnetic Co^{3+} (LS) in the layered structure.[12] In contrast, our nanosize $LiCoO_2$ exhibits a typical Curie−Weiss behavior for $T > 100$ K. The Curie constant was determined in the temperature range of 200−300 K. The Curie constant increases with decreasing particle size, and fitting of the Curie constant indicates that the molar Curie constant is as high as 0.20 in 10-nm-sized $LiCoO_2$ (details on the Curie constant fitting can be found in the Supporting Information, section S6).

Careful transmission electron microscopy (TEM) examination of the nanosized $LiCoO_2$ shows that all particles exhibit plate-like morphology, plates corresponding to the {001} planes; the edges are dominated by the {104} planes justifying our computational study of this surface (see TEM images in the Supporting Information, section S7). If the planes are terminated by the {001} surface, according to first principles computation of this work and previous work by Kramer and Ceder,[5] Co^{3+} remains octahedrally coordinated with a low-spin configuration. The contribution of Co^{3+} (IS) on the {104} and the Co^{3+} (HS) on the {110} surfaces are most likely attributing to the abnormally high magnetic susceptibility seen in nanosize $LiCoO_2$.

The proposed electronic spin state of the surfaces relevant for (de)intercalation has a significant impact on the lithium (de)intercalation voltage profile, as revealed by first principles computation performed to calculate the Li extraction potential from different surfaces. If Co^{3+} remains as LS on the {104} surface, the voltage of lithium extraction is as low as 2.32 V; by contrast, when a spin transition from LS to IS occurs, the voltage of lithium extraction is 3.69 V, close to the bulk value of 3.65 V. The narrowing energy gap between the occupied and unoccupied states in IS and

HS state Co ions indicates that the insulating nature of $LiCoO_2$ can be altered due to the change in spin state (see density of state plots in Supporting Information, section S9). This helps in explaining the fact that, in the lithium half-cell with nanosized $LiCoO_2$ as the cathode, a clear first-order phase transition, associated with the metal−insulator transition, is absent as no flat voltage plateau is observed upon the first charge15 (also see Supporting Information, section S8).

In conclusion, it is proposed in this work that electronic spin state transitions occur on the surfaces of stoichiometric $LiCoO_2$, where trivalent cobalt ions adjacent to the surface adopt an intermediate spin state if they are square pyramid coordinated and a high spin state if they are pseudotetrahedrally coordinated. This phenomenon is quantified in nanosized stoichiometric $LiCoO_2$. We also observed in first principles calculations that both {104} and {110} surfaces with optimized electronic spin states expand normal to the surface and the displacement is of the order of 0.1−0.2 Å. This work suggests that changes in electronic spin state could be a common phenomenon in transition metal oxides. The low coordinated geometries on the surface of the oxides result in spin states that are distinct from the bulk. Consequently, unique magnetic and electronic properties arise and alter the materials performance in devices. We show that, in this case, the voltage profile of (de)-intercalation is dramatically changed. It is therefore promising to control the surfaces and interfaces of nanosized materials to alter the electronic and magnetic properties, significantly different from the bulk behaviors.

■ ASSOCIATED CONTENT

Ⓢ Supporting Information

Computation and experiment details, fitting for Curie Constant, morphology, electrochemical measurement, density of states (DOS) plots. This material is available free of charge via the Internet at http://pubs.acs.org.

■ AUTHOR INFORMATION

Corresponding Author
shirleymeng@ucsd.edu

Notes
The authors declare no competing financial interest.

■ ACKNOWLEDGMENTS

■ REFERENCES

(1) Okubo, M.; Hosono, E.; Kim, J.; Enomoto, M.; Kojima, N.; Kudo, T.; Zhou, H. S.; Honma, I. *J. Am. Chem. Soc.* **2007**, *129*, 7444.
(2) Chen, H.; Grey, C. P. *Adv. Mater.* **2008**, *20*, 2206.
(3) Okubo, M.; Kim, J.; Kudo, T.; Zhou, H.; Honma, I. *J. Phys. Chem. C* **2009**, *113*, 15337.
(4) Levasseur, S.; Menetrier, M.; Shao-Horn, Y.; Gautier, L.; Audemer, A.; Demazeau, G.; Largeteau, A.; Delmas, C. *Chem. Mater.* **2003**, *15*, 348.
(5) Kramer, D.; Ceder, G. *Chem. Mater.* **2009**, *21*, 3799.
(6) Daheron, L.; Dedryvere, R.; Martinez, H.; Menetrier, M.; Denage, C.; Delmas, C.; Gonbeau, D. *Chem. Mater.* **2008**, *20*, 583.
(7) Ohzuku, T.; Makimura, Y. *Chem. Lett.* **2001**, 642.
(8) Daheron, L.; Martinez, H.; Dedryvere, R.; Baraille, I.; Menetrier, M.; Denage, C.; Delmas, C.; Gonbeau, D. *J. Phys. Chem. C* **2009**, *113*, 5843.
(9) Carlier, D.; Ménétrier, M.; Grey, C. P.; Delmas, C.; Ceder, G. *Phys. Rev. B* **2003**, *67*, 174103.
(10) Kim, J.; Middlemiss, D. S.; Chernova, N. A.; Zhu, B. Y. X.; Masquelier, C.; Grey, C. P. *J. Am. Chem. Soc.* **2010**, *132*, 16825.
(11) Mali, G.; Meden, A.; Dominko, R. *Chem. Commun.* **2010**, *46*, 3306.
(12) Kikkawa, S.; Miyazaki, S.; Koizumi, M. *J. Solid State Chem.* **1986**, *62*, 35.
(13) Buffat, B.; Demazeau, G.; Pouchard, M.; Hagenmuller, P. *Mater. Res. Bull.* **1983**, *18*, 1153.
(14) Demazeau, G.; Pouchard, M.; Thomas, M.; Colombet, J. F.; Grenier, J. C.; Fournes, L.; Soubeyroux, J. L.; Hagenmuller, P. *Mater. Res. Bull.* **1980**, *15*, 451.
(15) Chen, H.; Wu, L.; Zhang, L.; Zhu, Y.; Grey, C. P. *J. Am. Chem. Soc.* **2011**, *133*, 262.